Submitted to *Science*

Hexagonal Nanoporous Germanium through Surfactant-Driven Self-Organization of Soluble Zintl Clusters

Dong Sun, Andrew E. Riley, Ashley J. Cadby, and Sarah H. Tolbert*
Department of Chemistry and Biochemistry, University of California at Los Angeles, Los Angeles, California, CA 90095-1569

*to whom correspondence should be addressed: tolbert@chem.ucla.edu

Abstract: In this work we show that quantum-confined, nanoporous germanium can be produced by electrostatically driven co-organization of soluble Zintl clusters and organic surfactants. Low angle X-ray diffraction indicates that the material has a 2-dimensional hexagonal structure, and Ge EXAFS shows that after chemical treatment, the local structure is similar to bulk amorphous germanium. Nitrogen porosimetry indicates that the treated materials are porous with surface areas as high as 500 m^2/g. Moreover, the band gap of these nanoporous semiconductors can be tuned by changing the inorganic wall thickness, by adsorption of surface species in the pores, or by tuning the elemental composition of the inorganic framework. The results indicate that solution-phase templating can be used to synthesize periodic nanoporous versions of classic semiconductors with size and surface tunable optical properties.

Surfactant templating is a method that has been successfully employed to produce periodic inorganic structures for a wide range of oxide-based material.[1-5] In the synthesis, inorganic precursors co-assemble with amphiphilic organic species to produce structures with the periodicity of liquid crystalline phases, but with a rigid inorganic framework. If the framework is well connected, the surfactant can be removed by calcination or ion exchange to produce periodic porous inorganic materials, which can then be exploited for a range of size based adsorption applications such as catalysis or separations.[1,6,7] While these methods have proven highly versatile in the production of nanoporous oxides, electronic materials, particularly narrow band-gap semiconductors, appear to be much harder to access through these routes.

There has been incredible interest in nanoscale semiconductors over the past decade, in large part because quantum confinement has been shown to be a versatile method for tuning the

optical and electronic properties of a single material by using size.[8,9,10] Intense recent effort has been focused on moving away from simple layers, rods, or spheres to produce more complex geometries.[11,12] In keeping with this goal, many efforts have been made to apply the ideas of surfactant templating to semiconductor systems and some progress has been made. For example, a range of periodic surfactant/semiconductor or surfactant/metal composites have been produced by either liquid crystal templating,[13,14] electrochemical deposition,[15-18] or electrostatic co-organization.[19-24] Unfortunately, for virtually all of the semiconducting phases, the surfactant cannot be removed to produce porous materials, and so while complex semiconductor architectures can be produced, the semiconductor surface is not available to interact with other species in a way that could lead to sensors or other device applications.

One reason that nanoporous semiconductors are hard to produce via organic templating is that most semiconductors are crystalline, while almost all stable surfactant-templated materials are initially synthesized with amorphous frameworks. Crystalline materials are not generally flexible enough to form interconnected networks given the small radius of curvature found in templated solids. For some oxides, the frameworks can be crystallized after removing the surfactant,[4,25] but a stable, interconnected amorphous network is still required in the initial stages of the synthesis.

In our efforts to produce periodic nanoporous semiconductors, we have thus turned to a material that can display size controlled optical properties in the amorphous phase – the group IV materials. For example, quantum confinement has been demonstrated in amorphous Si/Ge multilayer structures (*a*-Si:H/*a*-Ge:H multilayers).[26,27,28] The challenge is to find ways to produce these group IV materials using a solution phase self-organization process. To do this, we utilize non-classical, reduced main group clusters called Zintl clusters as soluble inorganic precursors. Specifically, we use derivatives of the anionic truncated icosahedra Ge_9^{4-} cluster.[29] The use of Zintl clusters as precursors to nanoscale materials has already been established in the synthesis of group-IV nanocrystals based on these materials.[30,31,32] Most importantly for our application, because of the non-classical bonding, these clusters are redox active and so the cluster charge and association can be tuned through simple oxidation to move the system from

isolated Ge_9^{4-} clusters, to a $(Ge_9^{2-})_n$ polymer, and finally to neutral amorphous germanium.[33,34] In this work, we thus use electrostatic interactions to co-assemble soluble polymeric Ge Zintl clusters with cationic surfactants to form periodic templated germanium. With appropriate chemical treatment, we find that the Zintl clusters can be converted to zero valent Ge and the surfactant can be removed to produce periodic, nanoporous Ge.

In developing the self-organization chemistry of reactive non-oxide clusters, a number of synthetic challenges must be resolved. Foremost, while water is generally the solvent of choice for promoting amphiphilic assembly, it is far too reactive to use for any synthesis involving these Ge clusters. Formamide has been used in the past with anionic, non-oxide clusters,[20-23] but even this solvent is too reactive for the germanium system. To promote amphiphilic assembly, a network forming solvent is needed, and this network strength can be quantified using the Gordon parameter.[35,36] Water is clearly the best solvent for amphiphilic assembly with a value of 27.5; formamide is also quite reasonable with a Gordon parameter of 17.0.[36] For these experiments, we have employed ethylenediamine which has a Gordon parameter of only 10.4. Despite this lower value, we show that well ordered materials are produced. Ethylenediamine is unique in that it balances the need for donor-acceptor pairs (in this case N: and N-H) to promote assembly with the inability of reactive species to tolerate acidic protons. The use of this solvent may open up significant future potential for self-organization using highly reactive precursors.

In addition to the solvent, the surfactant must have an appropriate geometry to facilitate the formation of the desired phase, which in this case is a *p6mm* 2-dimensional hexagonal structure. It also must have an appropriate charge to interact favorably with the inorganic Ge cluster precursors. To satisfy the needed for strong attractive interactions, we use a cationic quaternary ammonium surfactant. To favor the formation of a curved phase like the hexagonal structure, we use a surfactant with a very large head group; specifically, we employ a cetyltriethylammonium bromide.[37] In the synthesis of Ge/surfactant composites, this surfactant is first dissolved in ethylenediamine and is then combined with a similar homogeneous ethylenediamine solution of the $(Ge_9^{2-})_n$ polymer.[38] While the cluster and surfactant concentrations are important, ordered composites can be synthesized using a fairly broad range

of absolute concentration and inorganic:organic ratios.[39] The polymeric, lower charge $(Ge_9^{2-})_n$ precursor is used rather than the monomeric Ge_9^{4-} for two reasons. First, the polymeric nature lowers the entropic penalty associated with the self-organization process. Second, the charge density on the $(Ge_9^{2-})_n$ polymer seems to be a good match for the charge carried by the organic surfactant when it is assembled into cylinders.[40]

Immediately upon mixing the surfactant solution and the Zintl cluster solution, a precipitate forms which produces the "as-synthesized" low angle X-ray diffraction pattern shown in figure 1 (solid line). The peak positions observed for this material show a 1:√3:2 pattern indicative of a *p6mm* hexagonal Ge/surfactant structure with a lattice constant of a = 4.15 nm. While low angle scattering can be used to characterize the nanometer scale order in these materials, high angle X-ray diffraction (not shown) indicates that these materials are completely amorphous on the atomic length scale. In agreement with the predictions of charge balancing, C, H, N, and Ge elemental analyses indicate a Ge_9 cluster:surfactant ratio of 1:2.07.

To characterize the local bonding in these composites, we utilized Ge EXAFS.[41] This technique is a sensitive probe of first and second shell bonding and allows us to understand whether our Ge_9 clusters survive into the hexagonal composite material. The data, presented in figure 2, a and b, show raw and Fourier transformed EXAFS collected on an as-synthesized composite. To fit the data, we make use of crystallographic data on the $(Ge_9^{2-})_n$ polymer (figure 2b, inset) to generate a model.[34] In this model, we consider the four unique sites of the $(Ge_9^{2-})_n$ polymer (indicated with dark shading). Because of the complexity of the model, we only include coordination distances up to 0.51 nm and thus we are unable to fit peaks at large radial distance. FEFF version 7 was used to generate phase and amplitude factors for each germanium site in a multiple scattering formalism,[42] and these were combined with appropriate weighting to generate an overall model for the data. The Debye-Waller factor, the relative bond lengths, and the exact edge position were then optimized to produce the best fit to the data (shown in figure 2b). While the agreement between the data and the fit is not perfect, there is good general agreement between all of the first four peaks of the model and the experimental EXAFS data. Given that the model is based on a regular crystal structure and that the composites are clearly amorphous,

the agreement is quite remarkable. Fairly small Debye-Waller factors of 0.0025 – 0.005 $Å^2$ also indicate that to a large extent, the Zintl cage structure is retained in the composite material.[43]

The existence of clusters in the composite indicates that the Ge walls are not well crosslinked. In agreement with this, any attempt to directly remove the surfactant results in complete loss of the nanometer scale periodicity as indicated by low angle X-ray scattering. By analogy with silica-based inorganic/organic composite materials, to produce a robust framework that can withstand the removal of the organic template, the framework must be well connected.[1] For silica, this entails dehydration to condense 2 Si-OH groups and form one Si-O-Si linkage. For the Ge system, the analogous chemistry would be the oxidative coupling of two anionic Ge species to form Ge-Ge bonds. Because of the high reactivity of the Ge clusters, we employ very mild oxidizing conditions. Ferrocinium hexafluorophosphate dissolved in acetonitrile was used to oxidize the anionic Ge toward neutral Ge and crosslink the framework. This choice of oxidant was made because of the inert nature of both the ferrocene product and the hexafluorophosphate ion.[44] Low angle X-ray diffraction (figure 1, dotted line) shows that the peak shifts toward higher *q* (smaller repeat distance) upon oxidation, indicating a more condensed network. Some disordering of the structure also occurs, however, as well resolved hexagonal higher-order diffraction peaks are no longer observed after oxidation. This process serves mostly to cross link the framework, rather than to remove the surfactant template as ^{13}C magic angle spin (MAS) solid-state NMR indicates that surfactant remains in the composite after oxidation.

To produce a porous material, the cationic surfactant must be replaced with a smaller cationic species, and the clear choice for this is a proton. In fact, in the absence of hydrogen, pure amorphous Ge is not stable. Theoretical studies have shown that 4-coordinate tetrahedral networks are overstrained and thus unstable.[45] In bulk materials, the average network coordination is significantly reduced by capping many germanium dangling bonds with hydrogen to produce *a*-Ge:H. Because of the highly reduced nature of our Ge starting material, we use H^+ rather than H_2 to generate this final hydrogenated structure, and thus we combine surfactant removal with dangling bond termination. Again because of the high reactivity of the Ge framework, the conjugate base of most acids can cause problems. To rectify this situation,

we utilize a supported acid (a proton exchange resin) to provide a proton source in the absence of both water and a reactive conjugate base.[46] Formamide was used as a solvent for the ion exchange because of the highly basic nature of ethylenediamine. While the precursor $(Ge_9^{2-})_n$ polymer is not stable in formamide, after oxidation with ferrocinium, little additional reaction occurs between the composite and the formamide.

The low angle X-ray diffraction pattern of the proton-treated composite in shown in figure 1, dashed line. A continued shift to higher *q* (smaller repeat distance) indicates some additional shrinkage of the composite upon surfactant removal. The final material shows a hexagonal lattice constant of 3.52 nm, although like the sample that was only oxidized and not proton treated, clear higher order hexagonal peaks still cannot be observed, indicating that the nanometer scale architecture is less ordered than the as-synthesized material. Comparison of the oxidized and oxidized/proton treated samples, however (figure 1), indicates that little additional disordering occurs upon proton treatment.

EXAFS analysis of data collected on the ferrocinium-oxidized proton-treated sample is shown in figure 2, parts c and d. The data shows a single sharp peak at short bond length and thus fits poorly with the cage model employed for the as-synthesized composite. This result clearly indicates that the Zintl cage structure has been removed by the oxidation and acid treatment. Previous work on bulk *a*-Ge:H has shown that this tetrahedral solid can be effectively fit with a first shell tetrahedral model.[47] Our composites can be fit extremely well with this same first shell tetrahedral model (Debey-Waller factor = 0.006 $Å^2$), suggesting that the local structure of the treated composites is very similar to bulk amorphous germanium. The presence of a small peak around $R + \delta \approx 4$ Å may also be related to some small amount of second shell tetrahedral Ge coordination. The results provide strong evidence that the Zintl based inorganic framework has been converted to simple amorphous Ge.

The porosity of the treated samples can be analyzed using nitrogen porosimetry.[48] The data in figure 3, which shows a classic type H4 isotherm,[49] was collected on a ferrocinium-oxidized, proton-treated composite that was washed with acetonitrile.[46] The isotherm shows a step at the nitrogen fragility point and as a result, the desorption step cannot be used to determine

the pore size distribution. Such an isotherm is usually characteristic of slit-like pores, rather than perfect cylinders.[50] In our case, this probably indicates that a small amount of surfactant remains in the pores. Despite this fact, the BET surface area is measured to be 500 m^2/g. Normalizing for the relative densities of silica and germanium, this value would correspond to ~1200 m^2/g surface area in a silica-based material, which is consistent with surfaces areas reported for highly ordered silica materials with similar repeat distances.[7] The results clearly indicate that the majority of the surfactant can be removed from these composites materials to produce porous, nanostructured germanium. While a range of well-ordered semiconducting surfactant/inorganic composites have been synthesized,[13,14,19-24] these Ge based materials are unique in that the surfactant can be removed without destroying the nanometer scale structure.

One of the main goals of producing a semiconducting phase is to provide a route whereby regular porosity can be combined with size tunable optical and electronic properties. Quantum size effects provide the main route to controlling these properties. We find that luminescence and absorption measurements on ferrocinium-oxidized proton-treated composites demonstrate that our materials do indeed show size-confined optical properties. Figure 4, top, shows three luminescence spectra from the composites.[51] The blue and the green traces were obtained on pristine nanoporous Ge samples and correspond to the in-phase and quadrature (out-of-phase) signals. Based on president from the literature, the faster, bluer, in-phase signal is assigned to luminescence from localized Ge-H sites at the pores surface,[52] while the longer lifetime, redder quadrature signal is associated with band edge luminescence from the Ge walls themselves.[26]

The position of this Ge luminescence peak is expected to shift inversely with the thickness of the Ge walls because of quantum confinement effects. As a result, we should be able to estimate a wall thickness by comparing the luminescence peak position to data collected on nanoscale germanium with a known thickness – in this case, we compare to *a*-Ge quantum wells. While it is not strictly legitimate to compare wall thickness in an interconnected hexagonal honeycomb structure to wall thickness in isolated flat quantum wells, the approximation is fairly reasonable. Comparing our luminescence peak position (1.3 eV) to trends established in a-Ge:H/a-Si:H quantum wells, we conclude that the final porous composites

have a wall thickness of ~1 nm.[26,28] This value is eminently reasonable given the position of the diffraction peaks, the size of the surfactant employed, and wall thicknesses observed in related silica based systems (usually ~1 nm). The observation lends strong credence to the postulate that our samples are behaving optically as simple quantum confined amorphous germanium.

If the sample is exposed to oxygen, the luminescence spectra changes dramatically. Figure 4, top, red curve, shows luminescence from such an oxidized sample. The strong luminescence peak at 2.0 eV can be related to GeO_x defects,[53,54] while the peak in the near IR is again assigned to luminescence from the *a*-Ge network itself. Such GeO_x defects are highly luminescent and tend to dominate any spectra. The complete absence of any GeO_x luminescence in our pristine nanoporous Ge indicates that indeed these samples are pure H terminated Ge.

Reflectance measurements can be used to calculate an optical band gap for these materials, and the results also show quantum confinement effects very similar to those seen in luminescence (figure 4, bottom).[55] The pristine material (green curve) shows an extrapolated absorption onset of 1.4 eV, a value that again corresponds to a wall thickness of ~1 nm when compared to the bulk *a*-Ge band gap of 1.0 eV.[26,27] The absorption is less prone than luminescence to spurious results based to low concentration defect sites, and so these results provide welcome confirmation that the amorphous germanium walls are acting as straightforward quantum-confined semiconductors.

We can also use reflectance measurements to show how this band gap can be tuned. For examples, the partly oxidized sample used for luminescence can also be subjected to diffuse reflectance measurements. We would expect this sample to show a bluer band gap as conversion of part of the 1 nm thick Ge wall to GeO_x should effectively reduce the *a*-Ge wall thickness. In agreement with this idea, the entire absorption spectrum is observed to shift to the blue.

In bulk semiconductors, surface band energies can also be shifted by binding molecules to the semiconductor surface.[56] Since our materials are essentially all surface, this type of binding can be used to cleanly shift the energy of the entire band edge absorption. For example, tetracyanoethylene (TCNE) has a moderately low LUMO.[57] If a pristine nanoporous composite is exposed to TCNE, the molecules can adsorb on the pore surface and the TCNE LUMO can

mix with the *a*-Ge conduction band. These two orbitals have fairly different energies, so the extent of mixing is small. Still, the mixing results in a lowering of the conduction band energy and thus a red-shift of the entire absorption spectra (figure 4, bottom, red trace). We note that the conductivity of simple semiconductor is exponentially dependant on the band gap, so small change in band gap should have a large effect on conductivity. The results thus suggest that this high surface area nanoporous Ge may find interesting sensor applications based on changes in optical or electronic properties upon analyte binding.

Finally, because of the flexible, non-classical bonding found in Zintl clusters, the chemistry presented here can be easily modified to include other elements. For example, instead of starting with a polymer based upon Ge_9 clusters, we can produce mixed Si/Ge clusters with composition $Ge_{9-x}Si_x$, where $x \approx 4$.[58] This material can be co-organized with surfactant, ferrocinium oxidized, and proton treated in exactly the same manner as the pure Ge system.[58] The result is a nanoporous Si/Ge alloy material that again shows a single peak in low angle X-ray diffraction and again shows a high surface area by nitrogen absorption analysis.[59] If the band gaps of this Si/Ge composite material is determined by diffuse reflectance (figure 4, bottom, purple trace), the absorption edge is observed to be significantly blue shifted. We anticipate that various alloys of Si, Ge, and Sn should allow for band gap tunability of periodic nanoporous materials through the visible red and hear IR regions.

These results show that it is possible to produce porous nanoscale semiconducting materials with a periodic interconnected framework and a large, accessible surface area. Furthermore, the optical properties of these materials can be tuned by changing the nanoscale dimension of the wall, the surface adsorbed species, or the atomic composition. The results show great promise for the use of surfactant directed self-organization in the production of periodic porous optical and electronic materials.[60]

Notes and References:

1. C.T. Kresge, M.E. Leonowicz, W.J. Roth, J.C. Vartulli, J. S. Beck, *Nature* **1992**, *359*, 710.
2. T. Sun, J.Y. Ying, *Nature* **1997**, 389, 704.
3. S. A. Bagshaw, T. J. Pinnavaia, *Angew. Chem. Intl. Ed. Engl*. **1996**, *35*, 1102.
4. P. Yang, D. Zhao, D. I. Margolese, B. F. Chmelka, G. D. Stucky, *Nature* **1998**, *396*, 152.
5. G. J. de A. A. Soller-Illia, A. Louis, C. Sanchez, *Chem. Mater*. **2002**, *14*, 750.
6. J.Y. Ying, C.P. Mehnert, M.S. Wong, *Angew. Chem. Int. Ed.* **1999**, *38*, 56.
7. K.W. Gallis, J.T. Araujo, K.J. Duff, J.G. Moore, C.C. Landry. *Adv. Mater.* **1999**, *11* , 1452.
8. C.B. Murray, D.J. Norris, M.G. Bawendi, *J. Am. Chem. Soc.* **1993**, *115*, 8706-8715.
9. A.A. Guzelian, J.E.B. Katari, A.V. Kadavanich, U. Banin, K. Hamad, E. Juban, A.P. Alivisatos, R.H. Wolters, C.C. Arnold, J.R. Heath, *J. Phys. Chem.* **1996**, *100*, 7212-7219.
10. W.L. Wilson, P.F. Szajowski, L.E. Brus, *Science* **1993**, *262*, 1242-1244.
11. L. Manna, D.J. Milliron, A. Meisel, E.C. Scher, A.P. Alivisatos, *Nature Mater.* **2003**, *2*, 382.
12. B. Mayers, Y.N. Xia, *Adv. Mater.* **2002** *14*, 279.
13. P.V. Braun, P. Osenar, S.I. Stupp, *Nature* **1996**, *380*, 325.
14. P.V. Braun, P. Osenar, V. Tohver, S.B. Kennedy, S.I. Stupp, *J. Am. Chem. Soc*. **1999**, *121*, 7302.
15. G. S. Attard, P. N. Bartlett, N. R. B. Coleman, J. M. Elliott, J. R. Owen, J. H. Wang, *Science* **1997**, *278*, 838.
16. G. S. Attard, S. A. A. Leclerc, S. Maniguet, A. E. Russell, I. Nandhakumar, P. N. Bartlett, *Chem. Mater*. **2001**, *13*, 1444.
17. P. A. Nelson, J. M. Elliott, G. S. Attard, J. R. Owen, *Chem. Mater*. **2002**, *14*, 524.
18. I. Nandhakumar, J. M. Elliott, G. S. Attard, *Chem. Mater*. **2001**, *13*, 3480.
19. M. J. MacLachlan, N. Coombs, G. A. Ozin, *Nature* **1999**, *397*, 681.
20. K. K. Rangan, S. J. L. Billinge, V. Petkov, J. Heising, M. G. Kanatzidis, *Chem. Mater*. **1999**, *11*, 2629.
21. P. N. Trikalitis, K. K. Rangan, M. G. Kanatzidis, *J. Am. Chem. Soc*. **2002**, *124*, 2604.
22. K. K. Rangan, P. N. Trikalitis, C. Canlas, T. Bakas, D. P. Weliky, M. G. Kanatzidis, *Nanoletters* **2002**, *2*, 513.
23. P. N. Trikalitis, K. K. Rangan, T. Bakas, M. G. Kanatzidis, *Nature* **2001**, *410*, 671.
24. A.E. Riley, S.H. Tolbert, *J. Am. Chem. Soc.* **2003**, *125*, 4551.
25. E.L. Crepaldi, G.J.A.A. Soler-Illia, D. Grosso, C. Sanchez, *New J. Chem.* **2003**, *27*, 9.
26. H. Deki, S. Miyazaki, M. Ohmura, M. Hirose, *J. Non-Cryst. Solids* **1993**, *166*, 841-844.

27. T. Tiedje, C.R. Wronski, P. Persans, B. Abeles, *J. Non-Cryst. Solids* **1985**, *77-78*, 1031.

28. H. Nakata, K. Murayama, S. Miyazaki, M. Hirose, *J. Non-Cryst. Solids* **2000**, *266*, 1067.

29. C. H. E. Belin, J. D. Corbett, A. Cisar, *J. Am. Chem. Soc.* **1977**, *99*, 7163-7169.

30. R. A. Bley, S. M. Kauzlarich, *J. Am. Chem. Soc*. **1996**, *118*, 12461.

31. B.R. Taylor, S.M. Kauzlarich, H.W.H. Lee, G.R. Delgado, *Chem. Mater*. **1998**, *10*, 22.

32. C.S. Yang, Q. Liu, S.M. Kauzlarich, B. Phillips, *Chem. Mater.*, **2000**, *12*, 983.

33. L. Xu, S.C. Sevov, *J. Am. Chem. Soc*., **1999**, *121*, 9245.

34. C. Downie, Z. Tang, A. M. Guloy, *Angew. Chem. Int. Ed.* **2000**, *39*, 337-340.

35. Defined as (surface tension)/(molar volume)$^{1/3}$, the Gordon parameter approximates the Gibbs free energy required to dissolve non-polar organic molecules into a solvent. J.E. Gordon, *The Organic Chemistry of Electrolyte Solutions*, (New York, Wiley, 1975).

36. D.F. Evans, D.D. Miller, "A Reappraisal of the Role of Water in Promoting Amphiphilic Assembly and Structure," *Water Science Reviews*, F. Franks (Ed.) **1989**, *4*, 1.

37. This surfactant can be synthesized from 1-bromohexadecane and triethylamine. For related syntheses, see F.M. Menger, C.A. Littau, *J. Am. Chem. Soc*. **1993**, *115*, 10083.

38. The germanium Zintl phase (K_2Ge_9) was synthesized from nominal ratios of elemental germanium (silicon) and potassium in a closed niobium under argon atmosphere. The solids were heated at 700 ºC for two days. In a typical synthesis of the nanocomposite, 0.4 gram of the solid K_2Ge_9 and 1.0 grams of dried tetraethylammonium bromide were dissolved into 10.0 mL of distilled ethylenediamine. The olive green supernatant, indicative of polymeric $(Ge_9^{2-})_n$, was then mixed with a solution containing 1.10 gram of the cationic surfactant cetyltriethylammonium bromide dissolved into 15.0 mL of distilled ethylenediamine.

39. D. Sun, A.E. Riley, S.H. Tolbert, to be submitted.

40. A. Monnier, F. Schuth, Q. Huo, D. Kumar, D. Margolese, R. S. Maxwell, G. D. Stucky, M. Krishnamurty, P.Petroff, A. Firouzi, M. Janicke, B. F.Chmelka, *Science* **1993**, *261*, 1299.

41. Data was collected on beamlines 4-1 and 6-2 at the Stanford Synchrotron Radiation Laboratory. Data was collected at temperatures below 100 K using either a liquid nitrogen or liquid helium cryostat. All data was collected in transmission geometry. Data analysis was performed using the EXAFSPAK software (http://www-ssrl.slac.stanford.edu/exafspak.html).

42. A. L. Ankudinov, B. Ravel, J. J. Rehr, S. D. Conradson, *Phys. Rev. B* **1998**, *58*, 7565; http://leonardo.phys.washington.edu/feff/.

43. B.K. Teo, *EXAFS: Basic Principles and Data Analysis* (New York, Springer-Verlag, **1986**).

44. For a typical oxidation reaction, 0.1 gram of ferrocinium hexafluorophosphate in 5.0 ml acetonitrile was added dropwise to an as-synthesized composite slurry in ethylenediamine (see

reference 38) under vigorous stirring. The mixture was stirred 0.5 - 1 hours and then was filtered under inert atmosphere. The dark reddish brown solid was washed with 10.0 ml of formamide.

45. A. R. Day, M. F. Thorpe, *J. Phys.: Condens. Matter* **1996**, *8*, 4389-4409; B. R. Djordjevic, M. F. Thorpe, *J. Phys.: Condens. Matter* **1997**, *9*, 1983-1994.

46. To proton treat the composite, the oxidized solid (see reference 44) was re-suspended in 20.0 ml of formamide. 1.0 gram of proton sponge [Acros, Amberlyst 15 (dry) ion-exchange resin] wrapped in Nylon cheesecloth was dipped into the mixture. This mixture was held at 90 ºC for ~12 hours. The red brown solid was filtered and then dispersed in 20.0 ml of acetonitrile. This mixture was kept at 60 °C overnight before filtration to isolate the final porous Ge material.

47. G. Dalba, P. Fornasini, M. Grazioli, *Physical Review B* **1995**, *52*, 11034-11043.

48. A Micromeritics 2010 porosimeter was utilized for these experiments.

49. S.J. Gregg, Sing, K.S.W, *Adsorption, surface area, and porosity, 2nd ed.* (London, Academic Press, **1982**).

50. J. C. P. Broekhoff, W. P. van Beek, *J. Chem. Soc. Faraday Trans. I* **1979**, *75*, 4255.

51. Samples were excited with 30 mW of light at 2.33 eV (532 nm) using a doubled Nd:YAG diode laser. Lock-in detection with a modulation frequency of 365 Hz was used to generate the in-phase and quadrature signals. All spectra were collected at 77 K.

52. G. Vogg, M.S. Brandt, M. Stutzmann, *Adv. Mater.* **2000**, *12*, 1278.

53. S. Miyazaki, K. Sakamoto, K. Shiba, M. Hirose, *Thin Solid Films* **1995**, *255*, 99.

54. Y. Kanemitsu, *Semiconductors and Semimetals,* Vol. 49 (San Diego, Academic Press, **1998**).

55. Reflectance UV/Vis-IR data was collected using a Shimadzu UV-3100 spectophotometer with an ISR-3100 integrating sphere attachment.

56. J.Z. Zhang, A.B. Ellis, *J. Phys. Chem.* **1992**, *96*, 2700.

57. V.G. Zakrzewski, O. Dolgounitcheva, J.V. Ortiz, *J. Chem. Phys.***1996**, *105*, 5872.

58. The Zintl compound $K_4Ge_5Si_4$ was prepared stoichiometrically from K, Ge, and Si using same procedure employed to produce K_4Ge_9. The synthesis of the mesoporous Ge/Si material also followed the same procedure utilized for the nanoporous germanium (references 38, 44, and 46) starting with 0.5 g of $K_4Ge_5Si_4$ and 3.7 g CTEAB.

59. The low angle XRD of the nanoporous Ge/Si shows a single peak at q = 0.196 $Å^{-1}$. Nitrogen porosimetry indicates a surface area 300 m^2/g.

60. This work was supported by the National Science Foundation (CHE-9985259) and by the Office of Naval Research (N00014-01-1-0757). This manuscript includes data collected at the Stanford Synchrotron Radiation Laboratory, which is operated by the Department of Energy, Office of Basic Energy Sciences. SHT is an Alfred P. Sloan Foundation Research Fellow.

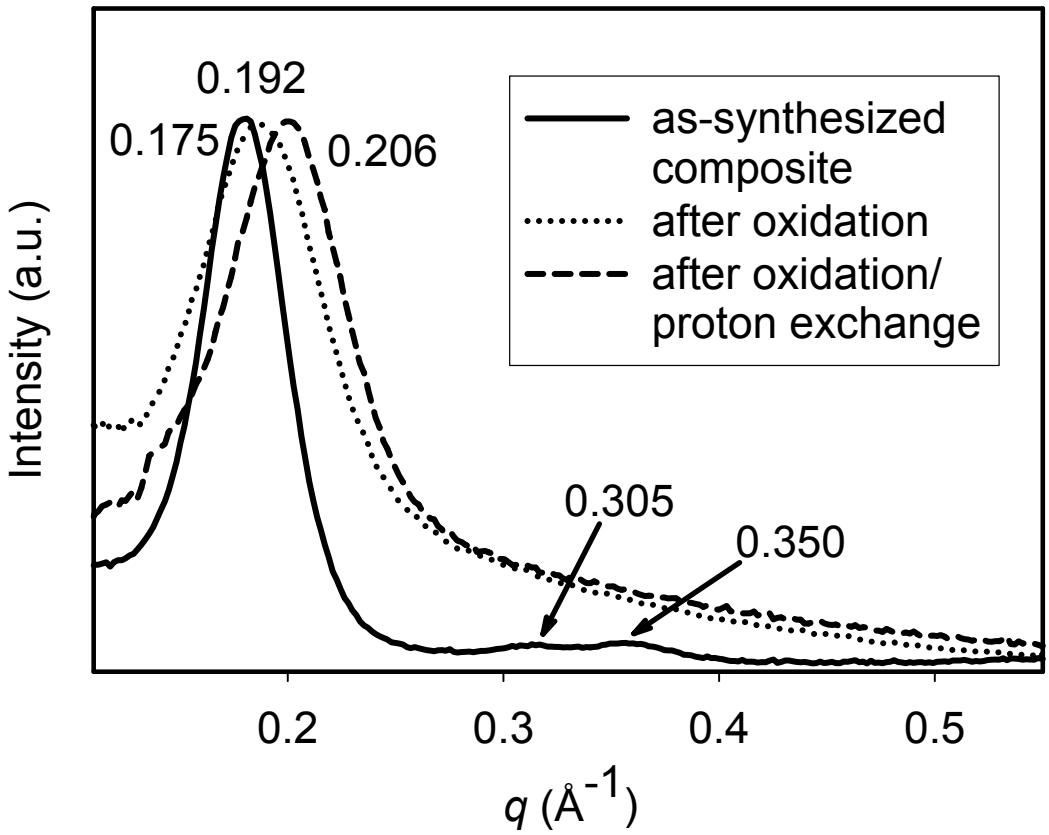

Figure 1. Low angle X-ray diffraction from germanium/surfactant composites after various chemical treatments. The as-synthesized composite (solid line) shows three peaks that can be indexed to a *p6mm* hexagonal phase. When this as-synthesized composite is oxidized (dotted line), only one clear peak is observed at larger q, suggesting that oxidation produces a more condensed but slightly less ordered framework. Further treatment with a proton exchange resin to produce a porous structure (dashed line), results in further shrinkage of the framework, but no additional disordering. The fit position of each peak in $Å^{-1}$ is indicated on the figure.

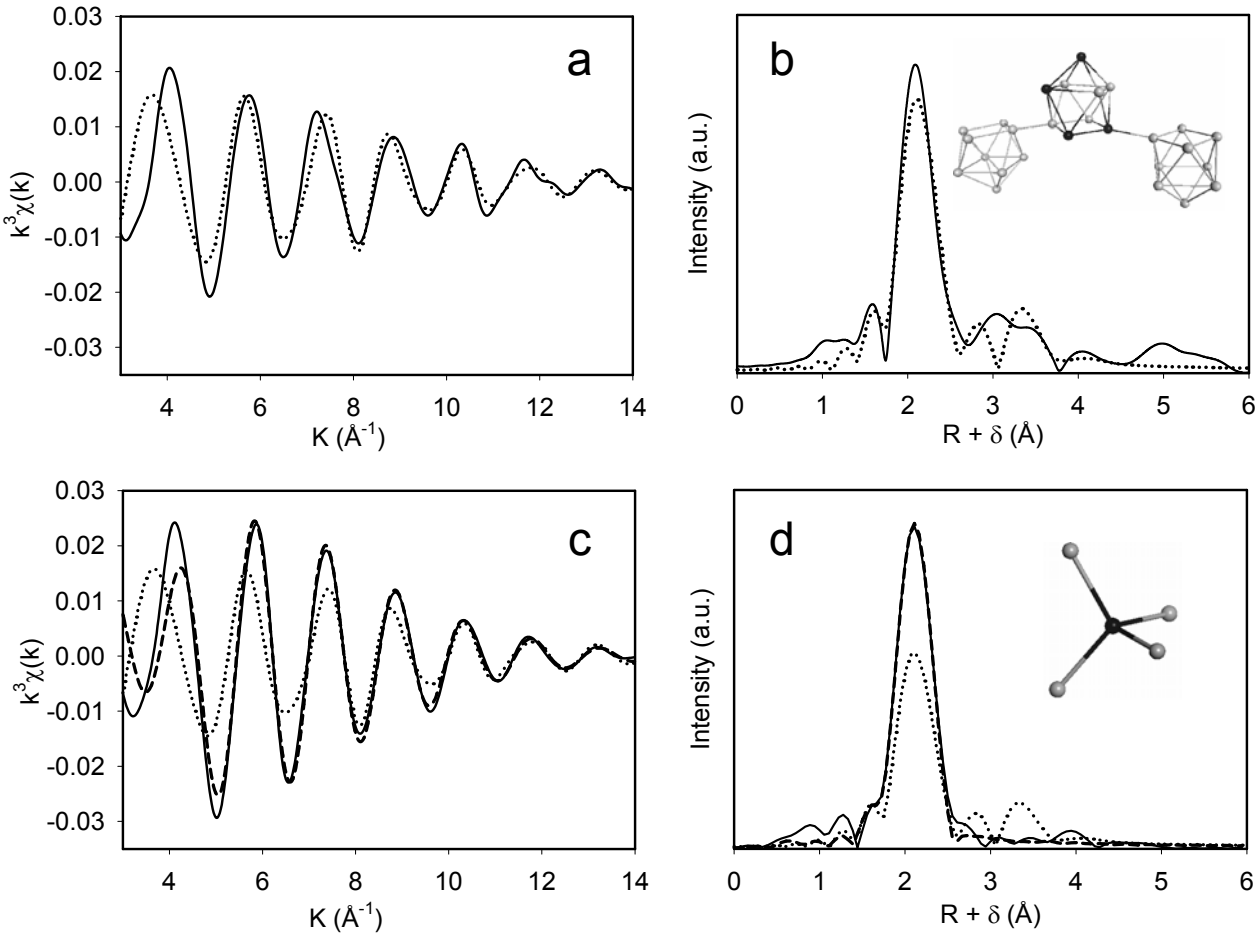

Figure 2. Raw and Fourier transformed Ge EXAFS obtained on surfactant templated germanium composites before (a and b) and after (c and d) chemical treatment. In all cases, solid lines correspond to the data, dotted lines correspond to a Zintl model generated using the cluster shown in part b, inset, and dashed lines correspond to a tetrahedral model generated using the cluster shown in part d, inset. In parts (a) and (b), the Zintl cluster model is shown to fit the data reasonably well, indicating that the icosahedral cage structure of the starting clusters is retained in the hexagonal surfactant templated composite. In parts (c) and (d), the data cannot be fit with the cluster model and instead can be well fit with a simple tetrahedral model. The results suggest that chemical treatment to oxidize the framework and remove the surfactant leaves the local structure similar to bulk *a*-Ge.

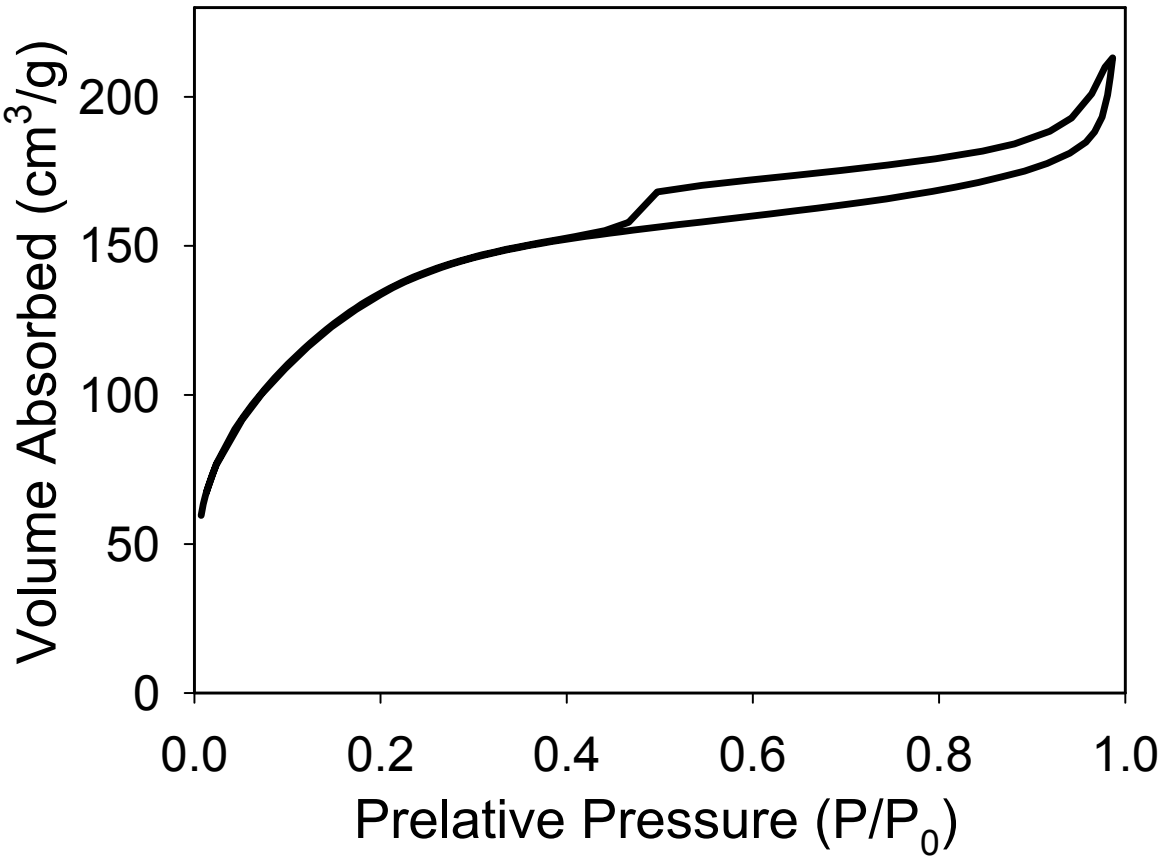

Figure 3. N_2 adsorption and desorption isotherms from mesoporous germanium obtained after ferrocinium oxidation, proton exchange, and an acetonitrile wash of a hexagonal germanium/surfactant composites. This type H4 isotherm is typical of slit-like pore. The material has a remarkably high surface area of 500 m^2/g.

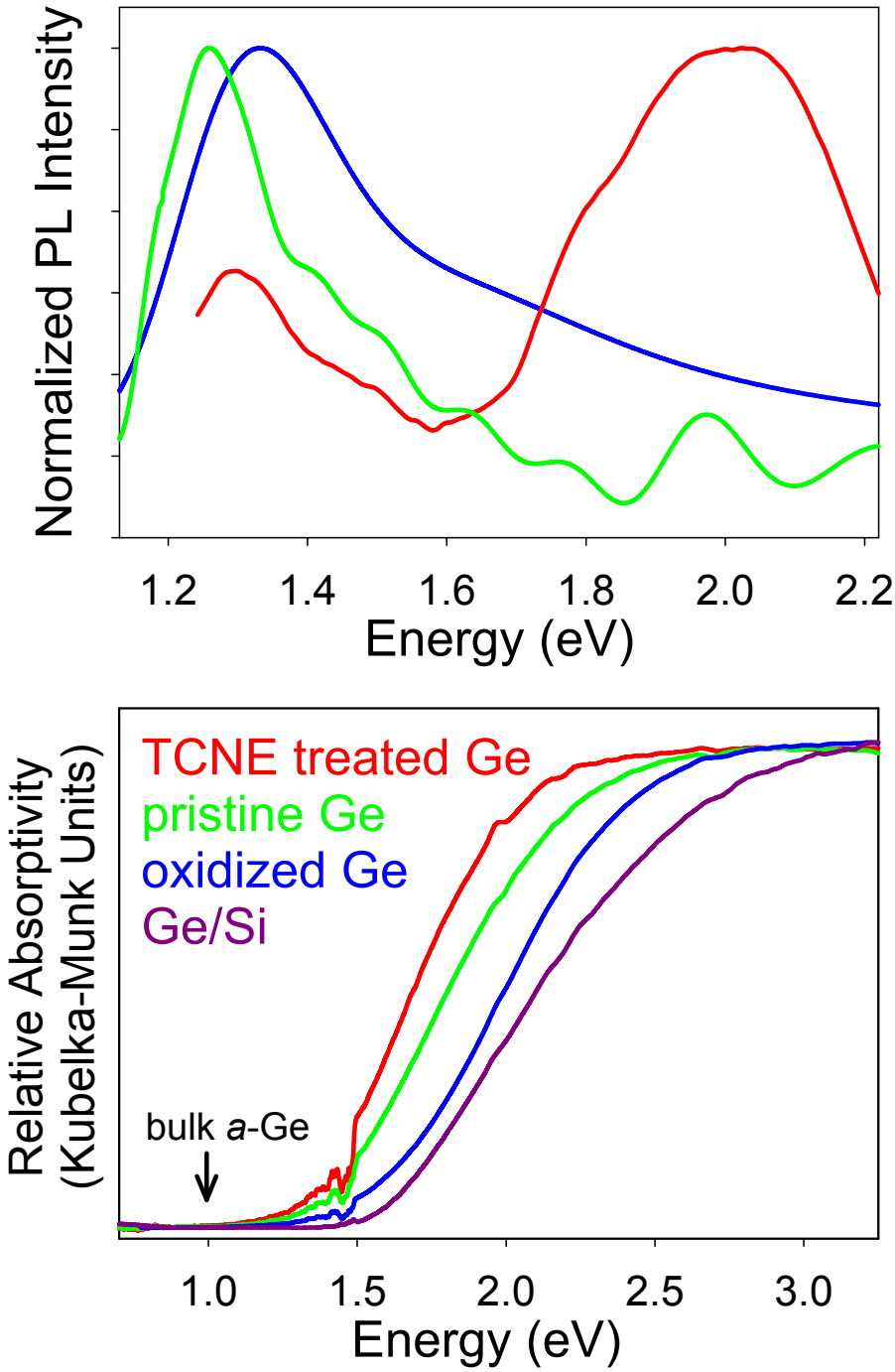

Figure 4. Photoluminescence (a) and near IR/UV-visible reflectance spectra (b) obtained on various nanoporous Ge based materials. For the luminescence data, the blue and green lines correspond to in-phase and quadrature data, respectively, obtained on pristing nanoporous Ge. The bluer in-phase peak corresponds to localized Ge-H sites, while the redder quadrature peak is consistent with ~1 nm thick quantum confined Ge. If the sample is oxidized in air, strong luminescence from GeO_x appears around 2 eV (red line). Reflectance data on pristine nanoporous Ge shows an extrapolated optical band gap of ~1.4 eV which is quantum confined with respect to bulk *a*-Ge. The band gap again corresponds to wall thickness of ~1 nm. The band gap can be shifted to the red by binding TCNE to the pore surface or shifted to the blue by oxidizing the walls to decrease there thickness. Materials with an even bluer band gap can be produced by using a mixture of Si and Ge in the walls.